Structural Engineering

A SURVEY OF PUBLICATIONS ON STRESS ANALYSIS OF HELICAL WIRES, OPTICAL FIBERS AND OPTICAL GROUND WIRES

By
Masoud Roshan Fekr

Report No. 97-12
January 1998

Department of Civil Engineering
and Applied Mechanics

McGill University
Montreal

A SURVEY OF PUBLICATIONS ON STRESS ANALYSIS OF HELICAL WIRES, OPTICAL FIBERS, AND OPTICAL GROUND WIRES

Masoud Roshan Fekr

Structural Engineering Report 97-12

Department of Civil Engineering and Applied Mechanics,
McGill University
Montreal, Canada

January 1998

TABLE OF CONTENTS

LIST OF FIGURES

LIST OF SYMBOLS

A	cross-sectional area of a wire
B	dimensionless bearing pressure
C_h	contact compliance between the helical wires and the compliant layer
D	pitch diameter of sheave
d	wire rope diameter
d_c	core wire diameter
d_h	helical wire diameter
E	modules of elasticity
E_o	modules of elasticity of a fiber in the region of very small strain
F_c	contact force between wires in different layers
F'_F	friction force per unit length of helical wire
F_R	radial force per unit length of a wire
F'_S	force acting on the core per unit length of helical wire
F_T	tangential force
F_t	axial component of the resultant force in a wire cross section
F'_{CF}	frictional force of core per unit length of core with no slip between wires
F'_{CAF}	frictional force of core per unit length of core with no slip between wires in the direction parallel to wire axis
F'_{CTF}	frictional force per unit length of core with no slip between wires in the direction tangential to wire axis
F'_{HF}	frictional force of helical wire per unit length with no slip between wires
F'_{HAF}	frictional force of helical wire per unit length with no slip between wires in the direction parallel to wire axis
F'_{HTF}	frictional force wire per unit length of helical wire with no slip between wires in the direction tangential to wire axis
f_{hc}	contact force exerted by compliant layer on a helical wire
G	shear modulus
H	components of internal moment resultant in t direction
I	second moment of area of the cross section of a helical wire
J	polar moment of inertia of the cross section of a wire
K_n	cable axial rigidity in non slipping part
l	length of a strand
L_T	transitional length
M	bending moment

M_b	components of internal moment resultant in b direction
M_n	internal moment in n direction
M_t	twisting moment
m	number of wires in cable
m_f	distributed friction torque related to the contact force between wires in different layers
N_b	component of internal force resultant in b direction
N_b^h	shear force component in b direction
N_n^h	shear force component in n direction
n	number of bends
P	axial load
P_n	interwire distributed forces in normal direction (per unit length)
Q	contact force per unit length between two adjacent wires
R	radius of the cylinder on which the center lines of the wires lie
r_h	radius of a helical wire
R'	final radius of a cylinder on which the center line of a helical wire lies
S_1	torsional stiffness of core wire
S_2	axial stiffness of core wire
S_3	bending stiffness of helical wire
S_4	torsional stiffness of helical wire
T	tension in wire rope
T_{out}	measured pulling tension
T_{in}	measured incoming tension
U	ultimate tensile strength of wire
W	occupancy or weight correction factor
X_h, Y_h, Z_h	external force components per unit length arise for equilibrium of the helical wire
α	lay (helix) angle of wires
α'	deformed helix angle
β	contact angle between line contact loads of two adjacent wires
δ	displacement in the axial direction
Δ	rotation around axis of the strand
ε	axial strain
ϕ	rotational strain of strand (rotation per unit length)
γ	normalized rotation of one pitch length of the strand ($\gamma = \Delta/2\pi$)
η	parameter of nonlinearity
φ	centerline twist of wires
κ, κ'	centerline components of curvature of wires

μ	effective coefficient of friction
ν	Poisson's ratio
ρ	radius of curvature of helical wire axis
ρ'	deformed radius of curvature of helical wire axis
σ_t	normal stress of wire cross section due to tension
σ_b	maximum bending stress
σ_c	stress in core
σ_C	maximum compressive stress due to contact
σ_o	stress in outer wires
τ	maximum shearing stress due to torsion
ξ	axial strain of helical wire

ABSTRACT

This paper is a survey of published studies on stress analysis and mechanical behavior of cables. Both theoretical and experimental investigations of cables composed of helical wires, optical fibers, and ground wires with optical fibers (OPGW) are presented. Also, the very first pioneering studies on stress analysis of cables are reviewed and discussed in detail.

1 HELICAL WIRES

1.1 Mechanics of wire ropes

Researchers and manufacturers have been interested in the design and analysis of wire ropes since the 1930's. Drucker and Tachau (1945) were the first researchers to attempt to find a structural design criterion for wire rope. They introduced a dimensionless bearing pressure B to select a wire rope:

$$B = \frac{2T}{UdD} \tag{1.1}$$

where T is the tension in the wire rope, U is the ultimate tensile strength of the wires, d is the diameter of the wire rope, and D is the pitch diameter of the sheave. Its significance was evident in the plot of life (number of cycles to failure) against this bearing pressure ratio B.

The failure of a wire rope was believed to be mainly as a result of fatigue and wear and not directly due to excessive axial stress in the rope. The conventional procedure of plotting the number of bends to failure against the average tensile stress T/A (where A is the cross-sectional area of the wire rope), the imaginary bending stress Ed/D (where E is the modulus of elasticity), and the sum of the two appeared to be improper considering the true cause of failure of the rope and widely scattered results. Drucker and Tachau proposed the nominal bearing stress (cross compressive stress) between a rope and a sheave, $2T/dD$, as a "reasonable selection criterion," since it creates high contact stresses and may increase the bending stresses and the friction between the wires. It was postulated that the distribution of tensile stresses in a straight wire rope, within some limits, was uniform and equal to the average stress T/A. It was also believed that the contact stress was independent of wire diameter and proportional to the square root of the bearing pressure. Experimental measurements of contact stress were close to the analytical prediction, however, the range covered for determining B was limited and insufficient for design purposes. The preliminary study of Drucker and Tachau motivated researchers to continue

investigating the complexity of the analysis and design of wire rope.

One of the earliest investigations on stress analysis in wires is the study of Hall (1951). In his paper, "*Stresses in Small Wire Ropes*," Hall disclosed that the necessity of calculating ultimate strength of cables used in aircrafts and control cables inspired him to investigate stresses in cables. He considered a wire rope made of several strands and each strand composed of wires as shown in figure 1.1. The strands and the wires were helically twisted around each other. Hall determined stresses on different parts of a wire rope by applying an axial load on the rope according to the following assumptions:

- the applied load was equally distributed amongst the strands and the wires in turn,
- there was neither friction nor bending in the wires and the strands,
- all strands and wires were tightly in contact with each other, such that only a static elongation of the rope would result from the loading.

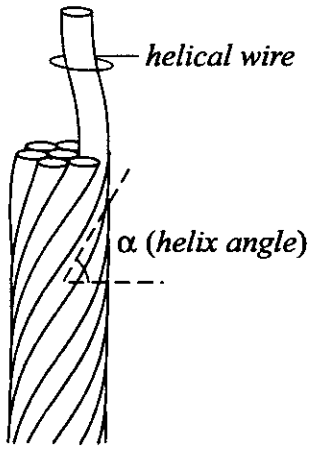

Figure 1.1 Typical wire configuration in a strand

However, many subsequent studies have revealed that these assumptions are unrealistic. Considering the wire rope as a fully coupled cross section and distributing the load equally amongst its components means neglecting the essential characteristics of a wire rope. Applying his theoretical model, Hall predicted that stresses in the outer wires would be notably higher than those on the inner wires, and consequently, that the outer wires would likely break under the applied load before the inner wires. It is clear that the radial forces applied by the wires on the strands and by the strands on the core have significant effects on the stresses in wire rope. Tangential forces generated from the axial load create a torque that changes the geometry of the strands and affects the stresses. Nevertheless, Hall's preliminary study revealed the complexity of stress analysis of wire ropes.

Six months after the release of Hall's article in *Wire and Wire Products*, Hruska (1951) published his paper titled "*Calculation of Stresses in Wire Ropes*" in the same journal. Hruska claimed that Hall made a "principle error" when he assumed that there was no friction in the wire rope. Hruska stated that the elongation of all wires, under the axial load, was the same due to the great friction between the wires. According to Hruska, an axial load on a wire rope produces three components of forces: axial tension force, radial force, and tangential force. His analysis of the axial tension showed that the core in a strand was always more stressed than the other wires, which is in contrast to Hall's prediction. He found that the stresses in the core, σ_c, and in outer wires σ_o, were related as

$$\sigma_c = \frac{\sigma_o}{\cos^2 \alpha} \tag{1.2}$$

where α is the lay (helix) angle of the wires.

Hruska (1952) published another article on the radial forces in wire ropes. He found that the radial forces increased with the lay angle, at the rate of $\tan\alpha \sin\alpha$, which yet had no effect on the axial forces. However, Hruska believed that the radial forces were important to consider when the core wire was worn or had a very small diameter, since in these situations, the strands which were not supported by the core would press each other. According to his analysis, the radial force F_R per unit length of a wire under an axial load P can be found as

$$F_R = \frac{P \sin^2 \alpha}{R} \tag{1.3}$$

where R is the radius of the cylinder on which the center lines of the wires lie (see Figure 1.2).

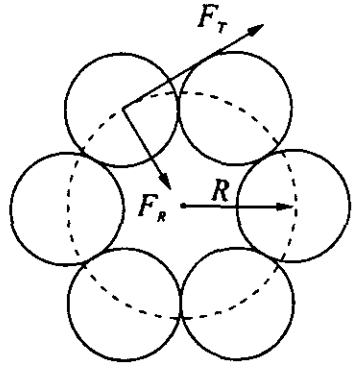

Figure 1.2 Radial and tangential forces on a wire rope cross section

Hruska (1953) also investigated tangential forces in wire ropes, and found that these tangential forces produced moments about the axis of the strand. He concluded that these tangential forces

and the resulting moments would either cause rotation of the wires in free-ends boundary conditions, or be the moment reactions of the supports if they were fixed. The tangential force F_T and the corresponding twisting moment M_t were determined as

$$F_T = P\sin\alpha \tag{1.4}$$

$$M_t = F_T R. \tag{1.5}$$

In the late 1950's, Leissa (1959), inspired by previous investigations on wire ropes, found that there was "no correlation between the fatigue life of a wire rope and either the direct tensile stress or the bending." However, there was a relation between the rope life and the contact pressure amongst wires. Leissa declared that the critical zones of stresses in a wire rope were the lines of contact along the core and the wire, and between two adjacent wires. He applied the "maximum-shear-stress" (Mohr-Coulomb) and the "maximum-normal-stress" (Rankine) failure theories to derive the relation between the axial tension force and the contact forces. Leissa concluded that the failure of brittle materials could be predicted by Rankine's theory while Mohr-Coulomb's was appropriate for ductile materials.

1.2 Stress analysis of helical wires

One of the first detailed study carried out on helical wires is the work of Machida and Durelli (1973). They derived linear expressions to determine the axial load, bending and twisting moments of helical wires, and the axial force and torsion of a core subjected to axial and torsional displacements. They believed that the analysis of a wire rope made of strands could be considered analogously to that of helical wires in a strand.

Machida and Durelli investigated three main static loadings, namely axial loading, torsion, and bending. Although they ignored the interwire contact deformation and Poisson's effect due to axial strain, they considered tensional loading and the combination of tensional and torsional loadings. According to their assumptions, two types of deformations could occur in a strand: a displacement in the axial direction, δ, and a rotation around the axis of the strand, Δ (see Figure 1.3). They categorized four types of loadings (axial force, bending, twisting and contact forces) associated with strains and stresses of the helical wire, and expressed all four types of loadings as a function of δ and Δ. On the basis of this study, the axial force P, the bending moment M, and the twisting moment M_t acting in a helical wire, and the resultant contact forces F_c acting on the helical wire can be found from the following equations:

$$P_h = A_h E(\varepsilon\sin^2\alpha + \gamma\cos^2\alpha) \tag{1.6}$$

$$M = \frac{2EI}{R}(\varepsilon - \gamma)\sin^2\alpha\cos^2\alpha \tag{1.7}$$

$$M_t^h = \frac{GJ_h}{4R}(\varepsilon - \gamma)\sin 4\alpha \tag{1.8}$$

$$F_c = \frac{P_h}{\rho'} \approx \frac{P_h}{\rho} \tag{1.9}$$

where;

A_h cross sectional area of a helical wire,

E Young's modulus,

I second moment of area of the cross section of a helical wire,

J_h polar moment of inertia of the cross section of a helical wire,

G shear modulus,

ε axial strain of the strand,

γ normalized rotation of one pitch length of the strand ($\gamma = \Delta/2\pi$),

ρ radius of curvature of the axis of helical wire,

ρ' deformed radius of curvature of the axis of helical wire.

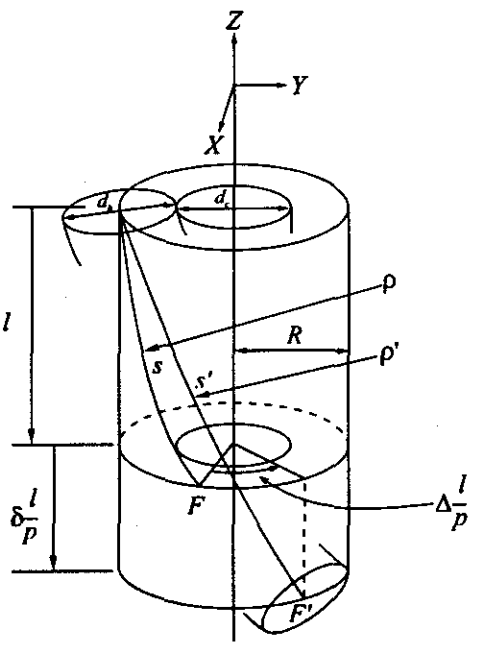

Figure 1.3 Axial displacement and rotation of a helical wire

Machida and Durelli also derived expressions for the external axial force and the torque of a strand made of six helical wires with a central core as follows:

$$P = P_c + 6P_h \cos\alpha' \tag{1.10}$$

$$M_t = M_t^c + 6(M_t^h \cos\alpha' - M\sin\alpha' + PR\sin\alpha') \tag{1.11}$$

where superscripts c and h denote the core and the helical wire, respectively. The deformed helix angle α', can be found as

$$\alpha' = \tan^{-1}\left(\frac{1+\gamma}{1+\varepsilon}\tan\alpha\right) \tag{1.12}$$

and for small deformation $\alpha' \approx \alpha$. Eqs. (1.10) and (1.11) can be expressed in terms of ε and γ, as follows

$$P = A\varepsilon + B\gamma \quad \text{and} \quad M_t = C\varepsilon + D\gamma \tag{1.13}$$

where:

$$A = A_c E + 6A_h E\cos^3\alpha$$

$$B = 6A_h E\sin^2\alpha\cos^4\alpha$$

$$C = 6A_h ER\sin\alpha\cos^2\alpha - \frac{3GJ_h}{2R}\sin 4\alpha\cos\alpha - \frac{12EI}{R}\cos^2\alpha\sin^3\alpha \tag{1.14a-d}$$

$$D = 6A_h ER\sin^3\alpha + \frac{3GJ_h}{2R}\sin 4\alpha\cos\alpha + \frac{12EI}{R}\cos^2\alpha\sin^3\alpha + \frac{2\pi}{p}GJ_c$$

They also investigated different end conditions of supports; such as axial loading with unrestricted ends (no torque is applied to the strand $M_t = 0$), torsional loading (no axial force is applied $P = 0$), and axial loading with restricted ends ($\Delta = 0$ or $\gamma = 0$). The results of a specific experimental analysis were presented to support their theoretical investigation.

As it can be seen, Machida and Durelli presented a rational model which took into account different possible loadings and the corresponding stresses. However, the important effects of friction amongst the wires, Poisson's effect, and the contact pressure between the core and wires, which can change the geometry, were all neglected in their model. It is noted that in their experimental work, an oversized epoxy model was used where the effect of friction was actually minimal. Despite its limitations, their work remains an important contribution as most subsequent investigations on helical wires have been based on this study.

Not long after Machida and Durelli, Phillips and Costello (1973) introduced a method to determine the stresses in twisted wire cables, with fewer limiting assumptions than previous researchers. They considered a cable as consisting of thin wires subjected to an axial force and a twisting moment with no friction between the wires. The general nonlinear equations for the bending and twisting of a thin rod subjected to line loads were solved using the six nonlinear

equations of equilibrium for each wire. In the stress analysis, they neglected the radial force exerted by the core on the wires because the core was relatively soft. An exact solution was presented to evaluate all stresses (axial, bending, twisting, and contact) in the wire. Each single wire in a cable was assumed to be subjected to an external bending moment and the tension T was considered constant along the length. The resultant axial force P and twisting moment M_t on the cable were determined by

$$P = m(T\sin\alpha' + N_b\cos\alpha') \tag{1.15}$$

$$M_t = m(H\sin\alpha' + M_b\cos\alpha' + TR'\cos\alpha' - N_bR'\sin\alpha') \tag{1.16}$$

where

m number of wires in cable,

T internal tension in the wire,

N_b component of internal force resultant in b (binormal) direction (see Figure 1.4),

M_b, H components of internal moment resultant in b (binormal) and t (tangential) directions, respectively,

R' final radius of a cylinder on which the center line of a helical wire lies,

α' final angle between the tangent to the center line of a helical wire and the plane normal to the axis of the helix.

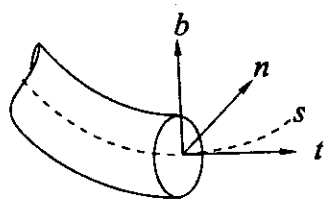

Figure 1.4. Normal (n), Binormal (b), and Tangential (t) directions at point in helical wire

The contact angle β, (see Figure 1.5) which locates the line of action of the line contact loads, Q, on a wire due to its neighbors is given by

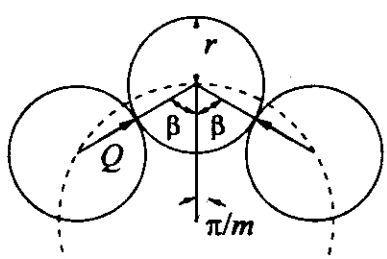

$$\beta = \sin^{-1}\left(1 + \frac{\sin^2\alpha}{\tan^2(\pi/2 - \pi/m)}\right)^{-1/2} \tag{1.17}$$

Figure 1.5. Contact between two adjacent helical wires

Phillips and Costello presented some numerical results for a few special cases. Given α' and T (obtained using a Newton-Raphson procedure to solve the nonlinear equations of equilibrium) the wire stresses can be calculated with equations (1.18 to 1.21)(see Figure 1.6). The normal stress of the wire cross section due to direct tension was given by

$$\sigma_t = \frac{T}{\pi r^2} \tag{1.18}$$

where r is the radius of the wire. The maximum bending stress σ_b and the maximum shearing stress τ due to torsion were given by

$$\sigma_b = Er\left(\frac{\cos^2\alpha'}{R'} - \frac{\cos^2\alpha}{R}\right) \tag{1.19}$$

and

$$\tau = Gr\left(\frac{\sin\alpha'\cos\alpha'}{R'} - \frac{\sin\alpha\cos\alpha}{R}\right) \tag{1.20}$$

respectively. The maximum compressive stress due to contact is

$$\sigma_C = -\sqrt{\frac{QE}{\pi R}} \tag{1.21}$$

in which Q is the contact force between two adjacent wires per unit length.

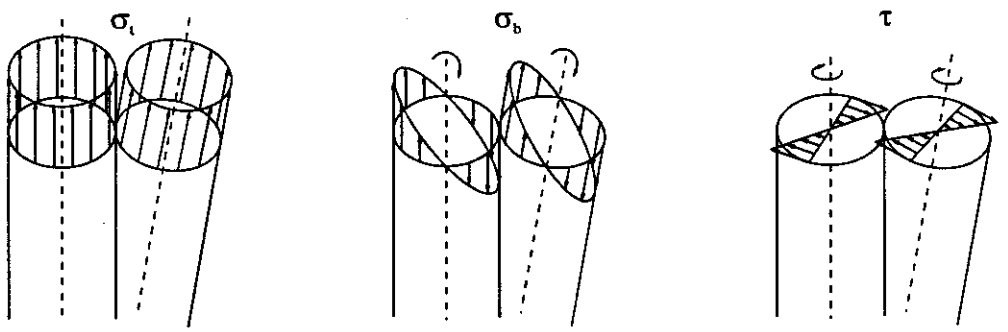

Figure 1.6. Normal stress (σ_t), Bending stress (σ_b), and Shearing stress (τ) in wires

This theoretical analysis is incomplete due to the neglect of frictional forces between the wires. The relative movements amongst the wires due to tension and twisting of the cable generate resisting forces that are closely related to the contact forces and stresses in the wires. Therefore, the friction forces can directly affect the stresses calculated by Phillips and Costello. On the other hand, if there is more than one layer of wires, which is a common situation, the friction and contact forces of wires with adjacent and lower wires, and also the friction between the wires and the core affect the stresses. The approach proposed by Phillips and Costello does not consider

the case of many layers of wires with a hard core. However, their investigation was the first to account for the contact forces and their interaction with other forces. Their study was not supported with any experimental work, which might have revealed important aspects that were not taken into consideration.

1.3 Advanced analytical and experimental studies of cables

The response of wire rope strands to axial tensile loads was more recently investigated theoretically and experimentally by Uttings and Jones (1987). They performed a series of tests on straight single steel strands of a seven-wire cable (a core with six wires, see Figure 1.7) subjected to static axial loads with different end restraints. They were the first to present a mathematical model considering the change of helix angle under load, Poisson's effects in wires, the effects of friction and wire flattening at the contact surfaces.

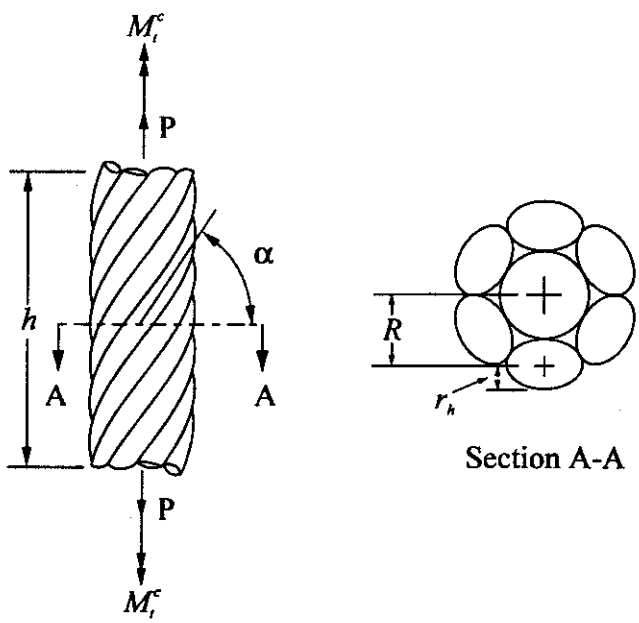

Figure 1.7 Geometry of a seven-wire strand

Moreover, Uttings and Jones conducted the first series of systematic experiments to determine the accuracy of their theoretical models, and to make comparison with previous theories presented by Machida and Durelli (1973), Phillips and Costello (1973), and Velinsky *et al.* (1984). Their experiments were carried out on a strand of 1.5 m length which was bent through 360° circular arcs of about 25-40 mm diameter in order to achieve efficient gripping at the supports. Under these conditions, the load-elongation behavior was nonlinear.

The resultant axial force and twisting moment were calculated using Eqs. (1.15) and (1.16) of the analysis by Phillips and Costello (1973), adding P_c and M_t^c to consider the contribution of the core, where

$$P_c = EA_c\varepsilon \quad \text{and} \quad M_t^c = EI_c\phi_c/(1+\nu) \tag{1.22}$$

are the core tension and twisting moment, respectively. The axial strain of the strand is

$$\varepsilon = (1+\xi)\frac{\sin\alpha'}{\sin\alpha - 1} \tag{1.23}$$

where ξ is the strain of helical wire axis, and the rotation per unit length ϕ_c is

$$\phi_c = \frac{R(1+\varepsilon)}{R'\tan\alpha'} - \frac{1}{\tan\alpha} \tag{1.24}$$

Neglecting wire flattening and Poisson's effects, the final helix radius R under all conditions of loading is

$$R = (d_c + d_h)/2 \tag{1.25}$$

where d_c and d_h are core wire and helical wire diameter respectively. Uttings and Jones considered some aspects of friction in their theoretical analyses, such as: Poisson's effect, zero friction between wires, friction with zero slip, and friction with some slip. They determined the helix radius of a strand under axial load (Eq. 1.26) considering Poisson's effect and the same modulus of elasticity for the core and helical wires.

$$R' = (1/2)\{d_c(1-\nu\varepsilon) + d_h(1-\nu\xi)\} \tag{1.26}$$

They took into account the wire flattening by imposing $\delta_Q = f(Q)$ as a flattening effect on the wire radius. Therefore Eq. (1.26) becomes

$$R' = (1/2)\{d_c(1-\nu\varepsilon) + d_h(1-\nu\xi)\} - \delta_Q \tag{1.27}$$

The wire flattening effect is determined empirically from experiments and considered as a function of Q, the contact force per unit length of helical wire. However, it is not clear how important the effect of contact force is on the reduction of the radius.

End effects were neglected in the previous analyses by Machida and Durelli (1973), Phillips and Costello (1973), and Velinsky *et al.*(1984). Uttings and Jones assumed that when there was no friction between the wires, any changes in the strand geometry occur over a transitional length L_T, at each end of the strand adjacent to the end grip. They postulated that when friction without slip was considered between wires, the frictional resistance from the core wire prevents some of

the rotation and bending of the helical wires about their axis. Furthermore, the friction force between the helical wire and the core was considered by treating each wire as a thin rod after Phillips and Costello (1973), and Love (1944).

A friction force per unit length of helical wire F'_F acts as shown in Figure 1.8 with components F'_{HTF} and F'_{HAF} which are tangential and parallel to the wire axis along the line of contact, respectively. The equal and opposite force acting on the core wire has two components F'_{CTF} and F'_{CAF}. Considering the core wire as a helical wire with $\alpha = 90°$, they calculated the total friction force on the core per unit length of core as

$$F'_{CF} = m\sqrt{\left(F'^{\,2}_{CAF} + F'^{\,2}_{CTF}\right)} \Big/ \sin\alpha \tag{1.28}$$

where,

F'_{CF} frictional force on the core per unit length of core with no slip between wires,

F'_{CAF} frictional force on the core per unit length of core with no slip between wires in the direction parallel to the wire axis,

F'_{CTF} frictional force per unit length of core with no slip between wires in the direction tangential to the wire axis.

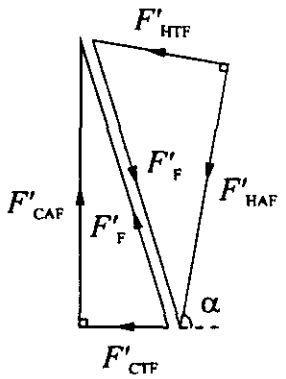

Figure 1.8 Interwire friction with no slip-forces

The frictional force acting on the helical wire per unit length is equal and opposite to the force acting on the core wire:

$$F'_{HF} = \sqrt{F'^{\,2}_{HAF} + F'^{\,2}_{HTF}} = \frac{F'_{CF}\sin\alpha}{6} \tag{1.29}$$

where,

F'_{HF} frictional force on the helical wire per unit length with no slip between wires,

F'_{HAF} frictional force on the helical wire per unit length with no slip between wires in the direction parallel to the wire axis,

F'_{HTF} frictional force on the helical wire per unit length with no slip between wires in the direction tangential to the wire axis.

By applying thin rod theory, Uttings and Jones calculated F'_{HAF} and F'_{HTF} as

$$F'_{HAF} = \frac{\left(M_b \mathrm{B}/S_3 - M_t^h \mathrm{A}/S_4\right)}{3d_h L_T\left(\mathrm{A}^2 - \mathrm{BC}\right)} \tag{1.30}$$

$$F'_{HTF} = \frac{\left(M_t^h \mathrm{C}/S_4 - M_b \mathrm{A}/S_3\right)}{3d_h L_T\left(\mathrm{A}^2 - \mathrm{BC}\right)} \tag{1.31}$$

where

$$\mathrm{A} = \sin\alpha\cos\alpha\left(1/S_2 - 1/S_1\right)$$
$$\mathrm{B} = \sin^2\alpha/S_1 + \cos^2\alpha/S_2 + 1/6S_4 \tag{1.32a-c}$$
$$\mathrm{C} = \cos^2\alpha/S_1 + \sin^2\alpha/S_2 + 1/6S_3$$

and,

M_t^h twisting moment about the axis of a helical wire,

S_1 torsional stiffness of the core wire, $S_1 = EI_c/\{r_c^2 \sin\alpha(1+\nu)\}$

S_2 axial stiffness of the core wire, $S_2 = EA_c/\sin\alpha$

S_3 bending stiffness of the helical wire, $S_3 = EI_h/r_h^2$

S_4 torsional stiffness of the helical wire, $S_4 = EI_h/\{r_h^2(1+\nu)\}$

L_T transitional length adjacent to strand termination.

They also concluded that if the friction between the core and the helical wires was insufficient to resist rolling contact, slip would occur. Therefore, slip occurs when the force acting on the core per unit length of helical wire F'_S is greater than the contact force Q per unit length of helical wire multiplied by the coefficient of static friction μ between the core and the helical wires. Uttings and Jones have modified the expression of Q given by Phillips and Costello concerning the reduced bending moment and torque in the helical wires in the presence of the friction. It should be noted that the theoretical analyses presented by Uttings and Jones do not account for more than one layer of helical wires. Also, the behavior will be even more complex if the core and the helical wires in different layers have different moduli of elasticity. Moreover, the large displacements of the wires and the core are not considered. In both of the analyses by Phillips and Costello (1973) and Uttings and Jones (1987), the cable is considered short and straight which is not appropriate in transmission lines and stayed bridges applications where the catenary configuration of the cable and the large displacements of the wires have significant effects on

cable stresses.

Uttings and Jones (1987-Part II) also compared their theoretical predictions with experimental results. Their experiments revealed that a single strand subjected to an axial load can be extended up to 2.3% more if taking into account Poisson's effects, friction, and wire flattening at the contact surfaces. In addition, the strand extension was greater under a given load with less torsional restraint on the supports. Their analytical model overestimated the measured torque generated in a strand under axial load and the torque was larger in strands with smaller helix angles. According to the mathematical model of Uttings and Jones, slip does not occur between the wires in a strand under axial load, except possibly in the transitional lengths near the strand ends. They realized that plastic yielding occurs at the contact surfaces and the effective point of contact in each wire moves without slip in the direction of the friction force acting on the wire. Therefore, contact between the core and each helical wire is no longer along a line. In addition, slip cannot be predicted in the presence of wire flattening which increases the contact area. They concluded that "whereas friction and wire flattening have very little effect on estimates of the overall strand response, the deformation of individual wires can be significantly affected by the magnitude of friction and contact forces and the proximity of strand terminations."

Raoof and Hobbs (1988) have proposed an analytical model for analysis of multi-layered structural strands. They presented several graphs to determine the interwire and interlayer contact forces. Each layer of wires in a multi-layered strand was treated as a statically indeterminate orthotropic cylinder with an equivalent modulus of elasticity. The analysis assumed that the wires in each layer just touch each other when there is no axial load on the strand and that strand was fixed against rotation at its ends. They determined the radial rigid body motion of the wires which would occur due to the change in lay angle in the absence of the central core. The radial force calculated agreed with the force determined by Hall (Eq. 1.3). They calculated the contact angle, β (see Figure 1.5) between the adjacent wires as

$$\beta = \sin^{-1}\left(1 + \frac{\cos^2\alpha}{\tan^2(\pi/2 - \pi/m)}\right)^{-1/2} \tag{1.33}$$

in which the changes in the lay angle and helix radius were ignored. A more exact method of calculating β was given by Costello and Phillips (1974) which is introduced in the next section (Eq. 1.71). In their work, Raoof and Hobbs implied that the interwire slip would not occur with "a small enough range to mean ratio of axial loadings,". However, full-slip occurs in case of

"large disturbances", hence, interwire friction forces were negligible compared to the change of the force in the wires. The modulus of elasticity for the full-slip and no-slip conditions was independent of the coefficient of friction μ. They presented that the ratio of $E_{\text{no-slip}}/E_{\text{full-slip}}$ is fairly constant for a practical range of mean axial load. The full-slip axial stiffness predictions were supported by experimental results on large diameter spiral strands with various diameters and lay angles of wire and strand.

The analysis of friction and wear in a wire rope was given analytical attention by Le Claire (1989). He addressed this problem to provide an upper bound estimate of the mechanical power transmission losses in a wire rope bent over a sheave. He postulated that the wires in a strand have no tendency to slide relative to one another under an axial load and the cross section of the strand remains plane, though distorted; likewise, the outer wires do not slide relative to the center wire or adjacent outer wires. As the strand is bent, however, relative motion can occur. Analytical results revealed that a wire rope in which the outer wires contact only the center wire (or layer beneath) and have a smaller diameter than the center wire, experiences a smaller mechanical power loss due to friction at the points of contact. He concluded that the above results indicate that contact occurs between adjacent layers but not between wires or strands in the same layer.

Le Claire (1991) also extended a linear theory for wire ropes that considered individual wire geometry and equilibrium including the effect of contact deformation between wires. After reviewing the approach of the axial response of a simple strand taken by Velinski et al. (1984) and Costello (1983), Le Claire extended the method to include the effect of contact deformation of a compliant layer. The cross section of a simple strand illustrated in Fig. 1.7 has a helix angle of α, measured from the perpendicular axis of the strand, and the helix radius, $R = r_h + r_c$, which locates the helical wire centerline. The components of curvature κ_h, κ'_h and twist φ_h, can be determined from Eqs. (1.34-1.35).

$$\kappa_h = 0 \quad \text{and} \quad \kappa'_h = \frac{\cos^2\alpha}{R} \tag{1.34}$$

$$\varphi_h = \frac{\sin\alpha\cos\alpha}{R} \tag{1.35}$$

The length h of the strand and the length l of a helical wire are related as

$$h = l\sin\alpha \tag{1.36}$$

The ends of the helical wire of length h make an angle of θ with the strand axis where

$$R\theta = l\cos\alpha \tag{1.37}$$

Under axial load, both the helix angle and the helix radius change by small amounts $\delta\alpha$ and δr. The corresponding change in lengths h and l, using Eq. (1.36) is

$$\delta h = \delta l \sin\alpha + l\cos\alpha\delta\alpha \tag{1.38}$$

and the corresponding change of θ given by Eq. (1.37) is

$$\delta\theta = \frac{1}{R}(\delta l\cos\alpha - l\sin\alpha\delta\alpha - \delta R\theta) \tag{1.39}$$

The corresponding change in the components of curvature and twist are

$$\delta\kappa_h = 0 \quad \text{and} \quad \delta\kappa_h' = -\frac{2\cos\alpha\sin\alpha}{R}\delta\alpha - \frac{\cos^2\alpha}{R^2}\delta R \tag{1.40}$$

and

$$\delta\varphi_h = \frac{\cos^2\alpha - \sin^2\alpha}{R}\delta\alpha - \frac{\sin\alpha\cos\alpha}{R^2}\delta R. \tag{1.41}$$

The axial strain of the strand and the helical wire are $\varepsilon = \delta h/h$ and $\xi_h = \delta l/l$ respectively. The Eqs. (1.38) and (1.40) relate these strains as

$$\varepsilon = \xi_h + \frac{\delta\alpha}{\tan\alpha} \tag{1.42}$$

The strand twist per unit length is $\phi = \delta\theta/h$, and Eqns. (1.36), (1.37), and (1.39) are combined to yield

$$\phi = \frac{1}{R}\left(\frac{\xi_h}{\tan\alpha} - \delta\alpha - \frac{\delta R}{R\tan\alpha}\right) \tag{1.43}$$

If the strand axial strain (ε) and twist per length (ϕ) are known , Eqns. (1.42) and (1.43) provide the helical wire axial strain (ξ_h), the change in helix angle ($\delta\alpha$), and the change in helix radius (δR). A third equation can be obtained by relating the change in helix radius to Poisson's effect in the wires as follows:

$$\nu_h r_h \xi_h + \delta R = -\nu_c r_c \varepsilon \tag{1.44}$$

where ν is Poisson's ratio. By using Eqns. (1.42) to (1.45), ξ_h, $\delta\alpha$ and δR can be determined. Meanwhile, Eqs (1.40) and (1.41) are used to find $\delta\kappa_h$, $\delta\kappa_h$, and $\delta\tau_h$. The bending moment components M_n^h, M_b^h and torque M_t^h which result on a cross section of a helical wire in response to these changes are

$$M_n^h = 0 \quad \text{and} \quad M_b^h = \frac{\pi E_h r_h^4}{4}\delta\kappa_h' \tag{1.45}$$

$$M_t^h = \frac{\pi E_h r_h^4}{4(1+\nu_h)} \delta\varphi_h \tag{1.46}$$

The shear force components N_b^h, N_n^h, the tension T_h, and the external force components per unit length X_h, Y_h, Z_h maintain the helical wire in equilibrium, where

$$N_n^h = 0 \quad \text{and} \quad N_b^h = M_t^h \frac{\cos^2\alpha}{R} - M_b^h \frac{\sin\alpha\cos\alpha}{R} \tag{1.47}$$

$$T_h = \pi E_h r_h^2 \xi_h \tag{1.48}$$

$$X_h = N_n^h \frac{\sin\alpha\cos\alpha}{R} - T_h \frac{\cos^2\alpha}{R} \quad \text{and} \quad Y_h = 0,\ Z_h = 0 \tag{1.49}$$

The strand axial force P and the twisting moment M_t required for the specified value of strand axial strain and twist per unit length, are found by summing the response of the m helical wires and center wire, as follows:

$$P = E_c \varepsilon \pi r_c^2 + m(T_h \sin\alpha + N_b^h \cos\alpha) \tag{1.50}$$

$$M_t = \frac{\pi E_c r_c^4}{4(1+\nu_c)} \tau + m(M_t^h \sin\alpha + M_b^h \cos\alpha + T_h R \cos\alpha - N_b^h R \sin\alpha) \tag{1.51}$$

Figure 1.9 shows the cross section of a wire rope with a compliant layer of thickness t_c. Neglecting contact deformations, this layer also effects the change in helix radius by its Poisson contraction and Eq. (1.44) can be written as

$$\nu_h r_h \xi_h + \delta R = -\varepsilon(\nu_c r_c + \bar{\nu}_c t_c) \tag{1.52}$$

where $\bar{\nu}$ is the Poisson's ratio of the compliant layer.

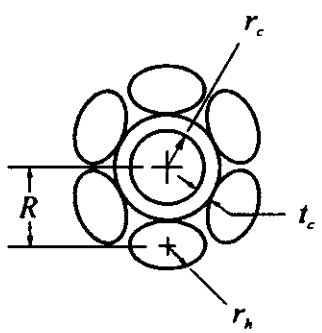

Figure 1.9 Cross section of a simple strand with compliant layer

In order to consider the contribution of contact forces, Le Claire added a term proportional to the contact force per unit length between the helical wires and the compliant layer to Eq. (1.52) as follows:

$$\nu_h r_h \xi_h + \delta R = -\varepsilon(\nu_c r_c + \bar{\nu}_c t_c) + C_h f_{hc} \tag{1.53}$$

where C_h is the contact compliance between the helical wires and the compliant layer, and f_{hc} is the contact force exerted by the compliant layer on a helical wire. If the modulus of the compliant layer is significantly less than the wire modulus, the effect of contact deformation on the change of the helix radius will be significant. Adding another layer of helical wires to the simple strand cross section (see Figure 1.10) makes it a complex strand.

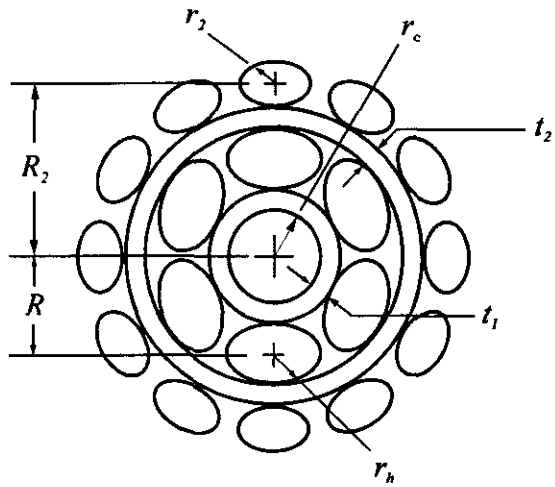

Figure 1.10 Cross section of two-layer strand with two compliant layers

Contact forces between wires result in deformations that reduce the helix radius of the wires in the strand and consequently reduce the equilibrium contact force per unit length and tension resulting in the wires. The deformations due to contact between wires of multilayered metallic strand are expected to be small, but should not be neglected. Moreover, multilayered cables used for signal transmission, often consist of several nonmetallic components and are subjected to unavoidable imposed strains. The deformations due to contact between the nonmetallic components may be significant and possibly beneficial due to the reduction in contact load and tension.

Le Claire extrapolated the results of one and two layers to a multilayered strand. For a strand with layer $i = 1,2,...,n$, where n is the number of layers, Eqs. 1.42, 1.43 and 1.53 become

$$\varepsilon = \xi_i + \frac{\delta\alpha_i}{\tan\alpha_i} \tag{1.54}$$

$$\phi = \frac{1}{R_i}\left(\frac{\xi_i}{\tan\alpha_i} - \delta\alpha_i - \frac{\delta R_i}{R_i \tan\alpha_i}\right) \tag{1.55}$$

$$\nu_i r_i \xi_i + \delta R_i = -(\nu_c r_c \varepsilon + \bar{\nu}_c t_c \varepsilon) - \sum_{j=2}^{i-2} (2\nu_j r_j \xi_j + \bar{\nu}_j t_j \varepsilon) + \sum_{j=2}^{i-1} C_j f_{j-1,j} \tag{1.56}$$

$$f_{i-2,i-1} = X_i + \sum_{j=i+1}^{n} \frac{m_j p_i \cos\bar{\alpha}_i}{m_i p_j \cos\underline{\alpha}_j} \left(\prod_{k=i+1}^{j-1} \frac{\cos\bar{\alpha}_k}{\cos\underline{\alpha}_k} \right) X_j \tag{1.57}$$

where $\underline{\alpha}_i = \tan^{-1}[p_i/2\pi(R_i - r_i)]$ and $\bar{\alpha}_i = \tan^{-1}[p_i/2\pi(R_i + r_i + t_i)]$.
and Eqs. (1.40 and 1.41) and (1.45-1.49) become

$$\delta\kappa_i = 0,\ \delta\kappa_i' = -\frac{2\cos\alpha_i \sin\alpha}{R_i}\delta\alpha_i - \frac{\cos^2\alpha_i}{R_i^2}\delta R_i \tag{1.58}$$

$$\delta\varphi_i = \frac{\cos^2\alpha_i - \sin^2\alpha_i}{R_i}\delta\alpha_i - \frac{\sin\alpha_i\cos\alpha_i}{R_i^2}\delta R_i. \tag{1.59}$$

$$M_{ni}^h = 0, \quad \text{and} \quad M_{bi}^h = \frac{\pi E_i R_i^4}{4}\delta\kappa_i' \tag{1.60}$$

$$M_{ti}^h = \frac{\pi E_i R_i^4}{4(1+\nu_i)}\delta\varphi_i \tag{1.61}$$

$$N_{ni}^h = 0, \quad \text{and} \quad N_{bi}^h = M_{ti}^h \frac{\cos^2\alpha_i}{R_i} - M_{bi}^h \frac{\sin\alpha_i\cos\alpha_i}{R_i} \tag{1.62}$$

$$T_{hi} = E_i \xi_i \pi R_i^2 \tag{1.63}$$

$$X_i = N_{bi}^h \frac{\sin\alpha_i\cos\alpha_i}{R_i} - T_{hi}\frac{\cos^2\alpha_i}{R_i},\ Y_i = 0,\ Z_i = 0 \tag{1.64}$$

Their results indicate that the presence of the compliant layer between wire layers reduces the tension experienced by the wires in the strand by at least one order of magnitude over the case in which the deformation is neglected or the compliant layer is absent. This effect is desirable in instrumental cables such as optical cables to preserve signal quality. Numerical results for three and ten-layer metallic strands indicate that neglecting contact deformations predicts greater wire tension and equilibrium contact force by 3% and 11% for the three and ten-layer strands, respectively.

1.4 Coefficient of friction of wires

Fee and Quist (1992) performed several tests to determine an effective coefficient of friction for

a cable pulled on top of an in-place cable (see Figure 1.11). They measured the cable pulling friction using a specially designed, multiple conduit bend apparatus. They considered that the coefficient of friction was dependent on conduit type, cable jacket type, lubricant presence and type, and normal pressure or sidewall pressure. They also developed a testing method to evaluate these parameters. All of the studies reported concerning the coefficient of friction indicate that the greater the normal forces between the cable and the conduit, the lower the effective coefficient of friction. The test was performed using a multi-bend apparatus in order to pull the cable through consecutive conduit bends, which produces rapidly increasing tension. The coefficient of friction was calculated by measuring the incoming and outgoing tensions, as

$$\mu = \frac{2}{Wn\pi} \ln\left(\frac{T_{out}}{T_{in}}\right) \tag{1.65}$$

Where

μ effective coefficient of friction,

n number of bends,

T_{out} measured pulling tension,

T_{in} measured incoming tension ,

W occupancy or weight empirical correction factor.

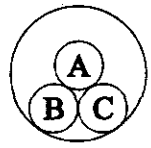

Figure 1.11 Cable A on top of in-place cables B or C

According to the experimental results, the coefficient of friction decreases as the incoming cable tension increases, in other words, as the sidewall pressure increases. Furthermore, the effective coefficient of friction for a nonlubricated cable was above 0.45, and it varied between 0.22 to 0.08 for a lubricated cable. On the basis of experimental results the weight correction factor (W) in Eq. (1.65) was found as

$$W = \frac{1}{\sqrt{1-\left(\frac{d'}{d+d'}\right)^2}} \tag{1.66}$$

where d and d' are the diameter of the upper cable (A) and the lower cable (B or C) respectively. Fee and Quist suggested a further study to understand the influence of normal pressure on the

effective coefficient of friction. They also concluded that a coefficient of 0.5 is conservative in calculations involving lubricated cables.

The effect of dry friction and interwire slippage in an axially loaded cable is addressed in the work of Huang and Vinogradov (1992). They defined the interwire friction as a local displacement of the wire surface with respect to the core or other wires. The cable composed of a core and n wires wound around it in such a way that each wire, in the first row, interfaces two adjacent wires and the core along the helix. Since the pretension load was large compared to the oscillating load, the interwire friction forces were determined by pretension load. They asserted that the interwire slippage could occur by the twisting and bending deformation of the wires. There were two types of contact between the wires: parallel contact between the wires of a same layer, and cross contact between the wires of different layers (see Figure 1.12). Huang and Vinogradov stated that, the distributed friction torque, m_f, is related to the contact force, F_c, between the wires in different layers, as

$$m_f = \mu F_c \tag{1.67}$$

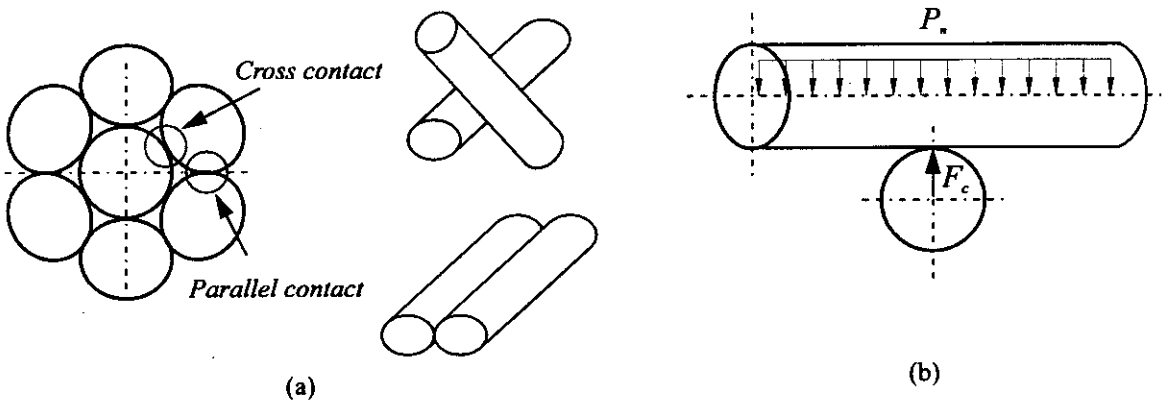

Figure 1.12 (a) Interwire contact and (b) Contact forces in cross touching

In case of cross contact, F_c was calculated from the equilibrium condition, as shown in Fig. 1.10, as

$$F_c = -P_n = \frac{P}{RK_n} E_h \pi r_h^2 \sin^4 \alpha \tag{1.68}$$

where P_n is the interwire distributed forces in the normal direction and can be presented approximately, using Love's (1944) equation of equilibrium,

$$P_n = \frac{F_n \sin^2 \alpha}{R} \tag{1.69}$$

in which F_n is the axial component of the resultant force in a wire cross section and is found from the geometry of the developed helix (Vinogradov and Huang, 1991),

$$F_n = \frac{P}{K_n}(EA)_h \sin^2\alpha \tag{1.70}$$

and K_n is the cable axial rigidity in non slipping part which is equal to,

$$K_n = (EA)_c + \frac{n(EA)_h}{\sin\alpha}. \tag{1.71}$$

For the parallel type of contact, the contact pressure is

$$F_c = -\frac{P_n}{2\sin\beta} = \frac{P(EA)_h \sin^4\alpha}{2RK_n \cos\beta} \tag{1.72}$$

where β is the contact angle as evaluated by Costello and Phillips (1974),

$$\cos\beta = \frac{1}{\cos\alpha}\sqrt{1 + \frac{1}{\tan^2(\frac{\pi}{m})\sin^2\alpha} - \frac{1}{\tan^2(\frac{\pi}{m})}\left(1 + \frac{1}{\tan^2\alpha \sin^2(\frac{\pi}{m})\left[\sin^2\alpha + c\tan^2(\frac{\pi}{m})\right]}\right) + \sin^4\alpha} \tag{1.73}$$

As expected, the contact forces are proportional to the axial load for both types of contact. Huang and Vinogradov (1994) also examined a cable as a system of helical wires and a core with distributed dry friction forces at the interfaces. In the analysis of the cable under a uniform bending moment, they found that there was a critical bending curvature when slip occurred between the wire and the core. They assumed small deformations theory and elastic material, and Poisson's effect in the wire was also neglected and only friction forces between the wires and the core were considered. The equations of a rod element derived by Love (1944) were used for the wires. Huang and Vinogradov claimed that slippage between wires was unlikely to occur when the bending deformation of the cable was small. This means that the interwire friction force is sufficient to hold the wires together and the cable behaves like a solid beam. In such a case, the corresponding bending rigidity was calculated as the sum of the second moments of area of all the individual wires of the cross section of the cable. They noted that with a large helix angle, the wires wound around the core had a nearly elliptical cross section. By increasing

bending, the interwire traction force increases and when it is equal to or larger than the friction force, slippage occurs. They concluded that with increasing bending, the slip spreads symmetrically from the neutral plane over the entire area of the cross section of the cable.

Huang and Vinogradov (1996) also studied the extension of the cable in the presence of dry friction. In the analysis of a cable under tension, they showed that slippage occurred due to the twisting and bending deformations of the cable. They asserted that due to the symmetry of the cable, neither the helical wire nor the core rotate at the middle section of the cable. However, far from the middle, as the twisting and bending stresses increase (due to increasing axial tension), the friction forces in the wire might be overcome, and slippage would take place. According to Huang and Vinogradov, two different slips occurred: a *micro-slip* and a *macro-slip*. The *micro-slip* occurred locally at the contact patch and the *macro-slip* took place along some length and was not uniform along the cable. The latter slip originated in the parts of the cable close to the ends and spread along some length towards the middle of the cable. They concluded that the elongation of the cable is nonlinear with the axial load, and that the energy dissipation due to dry friction is proportional to the cube of the tensile load and in inverse proportion to the friction forces, which is a typical characteristic of losses in dry friction joints.

Ura et al. (1991) have presented the friction properties of a wire rope for a cable puller when the rope is pulled. Experiments on three types of wire ropes revealed that a gripper with a curved surface created a large grasp force comparing to a flat gripper due to its greater contact surface. The coefficient of friction, which is here the ratio of pulling force to grasping force, had remarkable variations because of changing contact conditions. The results also showed that the radial displacements of the rope due to the compressive force of the gripper were much less than with the flat gripper. It was concluded that the real contact condition of the wire rope surface depends on the radial compressive load as well as the shape of the gripper.

2 OPTICAL FIBERS

2.1 Introduction

Optical fibers are widely used in telecommunication network systems. The low-loss and high-bandwidth transmission characteristics of optical fibers make them ideal for transmitting voice, data and video images. An optical fiber is composed of two main parts: an inner cylinder of glass which is called the core and a cylindrical shell of glass or plastic of lower refractive index called the cladding (Cherin, 1983). The core is typically made of a high-silica-content or multi-component glass. The cladding of the fiber is also made of a high-silica-content, multi-component glass, or plastic.

2.2 Mechanics of Optical Fibers

The study of the mechanical behavior of optical fibers is a specialty of optical fibers engineering. The number of studies related to the mechanics of fiber optics is small compared to other areas such as materials and manufacturing, but the proper modelling of the mechanical behavior of optical fibers is important in order to design fibers of optimal mechanical and optical performance. Suhir (1993) showed that the nonlinear stress-strain relationship of optical fibers, which was obtained experimentally under uniaxial tension by Mallinder and Proctor (1964), Krause *et al.* (1979) and Glaesemann *et al.* (1988), is also valid for compression and bending deformations, provided that the axial strains are not exceeding 5%.. He considered the effect of the material nonlinearity of optical fibers on the stability of short bare fibers, and also examined free vibrations of fibers subjected to tension and bending deformations with large deflections. The stress-strain relationship in optical fibers subjected to uniaxial tension (+) or compression (–) can be described as

$$\sigma = E_o \varepsilon (1 \pm \eta \varepsilon / 2) \qquad \varepsilon \leq 5\% \qquad (2.1)$$

where σ and ε are the stress and strain in the fiber, E_o is the initial modulus of elasticity of the fiber (*i.e.* in the region of very small strain, and η is the parameter of nonlinearity. For most optical fibers the Young's modulus is E_o = 72 GPa and the nonlinearity parameter is η = 6 . Suhir evaluated the buckling critical stress, thermal stresses and strains, and maximum stresses due to compression. He also assessed the effect of stress-strain relationship on the critical (buckling) stress in infinitely long dual-coated fibers, and in very short bare fibers. He concluded that in dual-coated fibers, the nonlinear stress-strain relationship results in a

significant reduction in the critical stress. Meanwhile, the strain corresponding to the critical stress was about 8% which was above the 5%. However, for a very short fiber, the material nonlinearity had a higher effect on the critical stresses and it should be considered.

Suhir (1995) also investigated the short-term and long-term durability of optical fibers. The evaluation of the short- and long-term reliability of the fibers and the adhesive and cohesive strength of the coating materials is done by *proof-testing*. It has been found (Krause, J. T. 1988, not reviewed by the author) that the specimen for *proof-testing* for a finite coating compliance can be sufficiently long for the optical fiber to be loaded to the same intensity as in an infinitely long structure.

2.3 Reliability of Optical Fibers

Szentesi (1986) has discussed the reliability of optical fiber cables considering the design and the characteristics of cables. He implied that cable failures were dominated by uncontrollable factors and the mechanical reliability is very high for the intrinsic cable and splices. The three important characteristics of optical fibers were discussed, namely their strength, attenuation, and microbending, all of which may be affected by environmental conditions. The behavior of optical fibers under tensile loading is nearly elastic and its failure is brittle. According to Szentesi, the strength of optical fibers is determined by randomly distributed surface defects, mostly due to mechanically or chemically induced cracks or flaws. The fracture probability is a function of fiber stress, fiber length, and time of loading which is modeled as a Weibull distribution. Szentesi declared that the attenuation of the fibers increases at the longer wavelengths due to the diffusion of the hydrogen into the glass core in hydrogen atmospheres. For example, single-mode fibers which slow long-term loss increments at 1 310 nm are expected to remain less than 0.02 dB/km after 25 years at 20°C in one atmosphere of hydrogen (Pitt and Marshall). The strength of an optical fiber is drastically affected by microbending, and fiber coating plays a dominant role in minimization of microbending. If a coating is deficient, degradation of microbending resistance or strength of the fiber is inevitable.

2.4 Optical Fiber Cables

Optical fiber cables are being used widely in communication networks. One possible structure of the optical fiber cables consists of several fiber optics inserted in a slotted rod, which is a load-carrying member located either at the core or around the optical fibers ribbons. A fiber ribbon consists of several coated optical fibers (see Fig. 2.1). Optical fiber ribbons are either tightly or

loosely inserted into helically shaped rectangular slots. The looseness of the fibers is created by the extra length of the fibers in the helical slots relative to the length of the cable. The dimensions of the slots are larger than the diameter of the ribbons, allowing for the additional length of the ribbon. If the cable is subjected to axial tension, the initial looseness of the fibers will prevent any fiber elongation (and stress) until the cable extension becomes equal to the initial fiber overlength.

Hatano *et al.* (1986) investigated theoretically and experimentally the structural design of a new type of cable assembly with several optical fibers tightly inserted into slots (Figure 2.1). They claimed that such a cable has many advantages such as compactness, high controlling of fiber strain and protection of fibers from lateral forces. The latter is achieved by freeing the movement of the ribbons along its axis when the cable is bent.

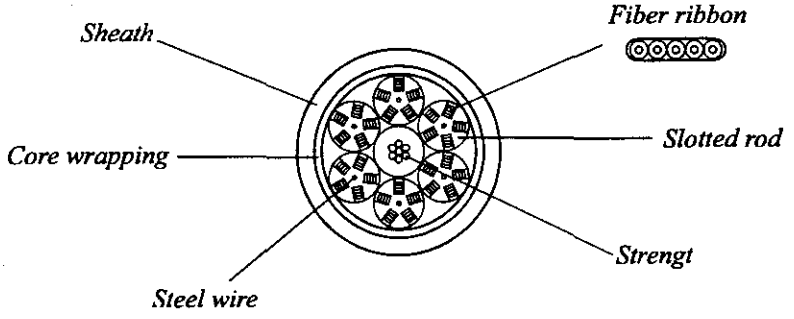

Figure 2.1 A typical cable with optical fibers

The design of the coating and slot structures were optimized to minimize the tensile force on the fiber ribbons. Hatano *et al.* also took into consideration bending, twisting as well as residual strains in optical fibers during cable manufacturing and installation. They measured optical losses at each stage of the manufacturing process and after installation in the field. These measurements showed the excellent performance during manufacturing. Also, the measured optical losses after installation were satisfactory.

3 GROUND WIRE WITH OPTICAL FIBERS (OPGW)

3.1 Introduction

Overhead ground wires with optical fibers (OPGW) are used widely in transmission lines. The primary function of the ground wire is to protect the line electrically against lightning, while optical fibers incorporated in the core of the cable serve a telecommunication purpose. Traditional ground wires are composed of helical galvanized steel strands. In recent years, the traditional ground wires have been replaced with ground wires carrying optical fibers which are protected inside the cable core. In most constructions, the fibers are designed to be stress free or to resist only low stresses under normal operation loads.

The structure of optical fiber cables typically consists of several fiber optics arranged in ribbons or strands, which are either tightly or loosely inserted into helically shaped slots on an aluminum spacer. The relative looseness of the fibers is created by the extra length of the fibers compared to that of the cable. The large diameter of the slots with respect to the diameter of the fiber ribbons or strands allows for the additional length of the fibers, which is also referred to as excess length or overlength. Due to compatibility of strains and displacements, the optical fibers will not experience any elongation and stress until the overall cable extension equals the fiber overlength.

3.2. Mechanics of an OPGW

Russ et al. (1986) investigated the optical and mechanical characteristics of an OPGW. Several experiments were performed to assess the characteristics of the OPGW such as attenuation changes due to heat cycling at low and high temperatures, creep, tensional behavior, and performance in simulated short-circuit tests. The OPGW tested was composed of an optical fiber unit surrounded by an aluminum tube covered with one or more layers of aluminum clad steel strands (Figure 3.1). The fibers are tightened with a filling compound which restraints fiber movements, microbending, and local pressure against the fibers under various loads. Two typical constructions were tested, namely the loose tube construction and the tight tube construction.

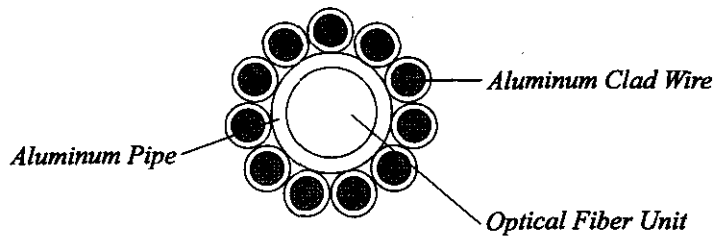

Figure 3.1 Cross section of the OPGW tested by Russ *et al.*

For the loose construction, Russ et al. verified that under the uniaxial tension test, no attenuation was generated when the cable extension remained below the initial fiber overlength. However, the attenuation increased drastically for extensions in the excess of the overlength because the fibers are then unrestrained. Conversely, no attenuation loss was measured in the tight construction before the cable failure.

The only detailed three-dimensional finite element modeling study of an OPGW reported in the literature is the work of Abé *et al.* (1989), which was restricted to the study of a grooved aluminum spacer (slotted rod) as illustrated in Figure 3.2 and summarized below. The optical fiber unit was a loose-type and was composed of 600 optical fibers arranged in a ribbon structure. The forces and bending moments in the slotted rod of an optical fiber cable were determined using Love's equilibrium equations (1944). The deformations of the slotted rod subjected to forces and bending moments were derived using a three-dimensional finite element model. The results showed that for the particular cable studied, the deformations of the slotted rod were very small: it was concluded that for an extensional strain of 0.1% and a bending curvature of 1/1100 mm^{-1}, the clearance between the fibers and the lateral wall of the slot was sufficient to meet the design criteria. It should be emphasized that this study was limited to an isolated slotted rod without considering the other components of the optical fiber cable, *i.e.* neither the external metallic envelope nor the optical fibers inserted in the slots.

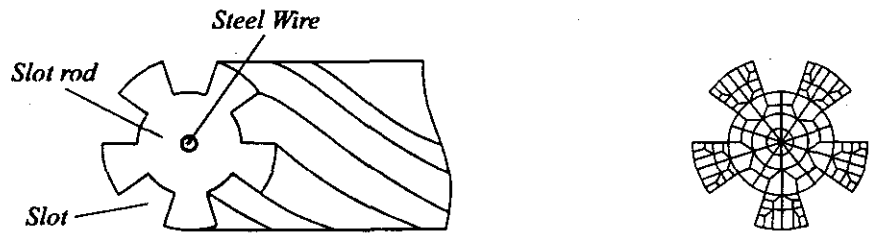

Figure 3.2 Cross section of aluminum spacer (slotted rod) adapted from Abé *et al.*(1989)

3.3 Mechanical Reliability of OPGW

Savadjiev and McComber (1995) have investigated the reliability of a typical loose construct OPGW used in cold climatic regions prone to atmospheric icing. As experienced in the recent freezing rain storm in Eastern Canada, ice accretions can be sufficient to fail individual cable components (aluminum wire or optical fibers) or even the whole OPGW. A statistical approach was used for all random factors to determine the behavior of the real line cables. Using Monte Carlo statistical trials technique, they concluded that the optical fibers had a lower reliability than the metallic strands. They suggested that this reliability could be improved with a relatively small increase in the depth of the spacer helical groove.

3.4 Detailed Study of the Mechanical Behavior of OPGW

The complex cross section of an OPGW makes it difficult to understand its behavior under various types of loadings, and more sophisticated analysis than that presented in this review is necessary to advance knowledge in this field. Consequently, the author is currently conducting a detailed study of the mechanical behavior of an OPGW using state-of-the art finite element modeling (ADINA, 1997). The OPGW investigated is a loose type construction manufactured by Phillips-Fitel at its Rimouski plant and used widely by Hydro-Québec on its overhead transmission network (see Figure 3.3). The scope of the study is to model the mechanical behavior of the optical ground wire (OPGW) used in overhead transmission lines, in order to predict the stress state in the optical fibers and as a result, estimate the opto-mechanical reliability of the cable under various loads.

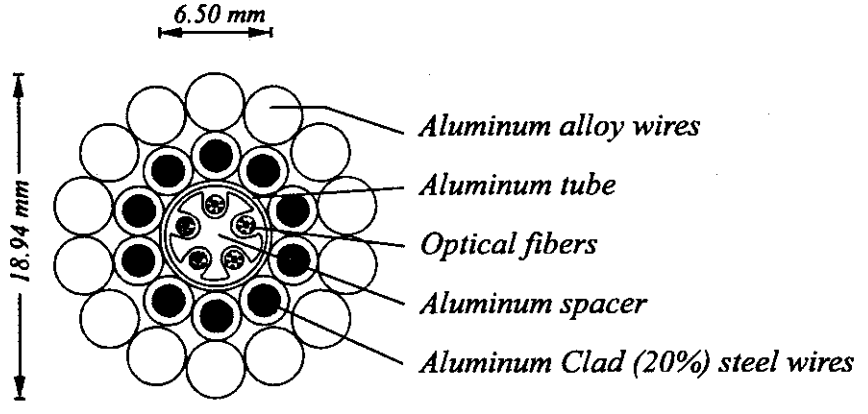

Figure 3.3 Cross section of the OPGW used by Hydro-Québec

It is noted that results of the numerical model will be verified using the results of mechanical tests carried out at Hydro-Québec's research facilities (High Power Laboratory and full-scale experimental line) in Varennes, Canada.

BIBLIOGRAPHY

Abé, H. , Kusumi, Y. , Saka, M. 1989. "Deformation of slot rods in a slot-type optical fiber cable," *Nippon Kikai Gakkai Ronbunshu*, a Hen. Vol. 55, No. 514, pp. 1462-1468. (Paper in Japanese with abstract in English).

ADINA, R & D, Inc., 1997. *ADINA - A Finite Element Program for Dynamic Incremental Nonlinear Analysis, Theory and Modeling Guide,* Report ARD 97-9, Watertown, MA.

Bacon, F. and Maklad, M. S. 1994. "Long-term mechanical reliability of single mode optical fibers," *Proceedings of SPIE-The International Society for Optical Engineering,* Society of Photo-optical Instrumentation Engineers, Bellingham, WA, USA. Vol. 2292, pp. 340-352.

Barnoski, M. K. 1981. "Fundamentals of Optical Fiber Communications," *Academic Press Inc.*

Blau, P. J. 1996. "Friction science and technology," *Marcel Dekker, Inc.*

Cherin, A. H. 1983. "An introduction to optical fibers," *McGraw-Hill Book Company.*

Costello, G. A. 1978. "Analytical investigation of wire rope," *Applied Mechanics Review*, Vol. 31, No. 7, pp. 897-900.

Costello, G. A. 1983. "Stresses in Multilayered Cables," *Journal of Energy Resources Technology,* Vol. 105, pp. 337-340.

Costello, G. A. and Phillips, J. M. 1974. "A more exact theory for twisted wire cable," *Journal of the Engineering Mechanics Division, ASCE*, Vol. 100, pp. 1096-1099.

Drucker, D. C. and Tachau, H. 1945. "A new design criterion for wire rope," *Journal of Applied Mechanics, Transactions. American Society of Mechanical Engineering.* 67, pp. A-33 - A-38.

Fee, J. M. 1994. "Pulling tension calculation program which allows coefficient of friction to vary continuously with cable sidewall pressure," *Proceedings of the IEEE Power Engineering Society Transmission and Distribution Conference.* pp. 314-316.

Fee, J. M. and Quist, D. J. 1992. "A new cable pulling friction measurement method and results," *IEEE Transactions on Power Delivery*. Vol. 7, No. 2, pp. 681-686.

Fee, J. M. and Solheid, D. P. 1994. "Coefficient of friction effects of polymers, silicone oil, and mini-rollers in cable pulling," *Proceedings of the IEEE Power Engineering Society Transmission and Distribution Conference. Published by IEEE, IEEE Service Center, Piscataway, NJ, USA*. pp. 317-322.

Hall, H. M. 1951. "Stresses in small wire Ropes," *Wire and Wire Products*, Vol. 26, pp. 228, 257-259.

Hatano, S., Katsuyama, Y., Kokubun, T., and Hogari, K. 1986. "Multi-hundred-fiber cable composed of optical fiber ribbons inserted tightly into slots," *Proceedings of 35th International Wire and Cable Symposium,* Published by US Army Communications-Electronics Command, Fort Monmouth, NJ, USA. pp. 17-23.

Hayata, K., Koshiba, M., and Suzuki, M. 1987. "Stress-applied optical fiber having inhomogeneous core," *Electronics and Communications in Japan, Part2: Electronics,* Vol. 70, No. 9, pp. 74-81.

Hruska, F. H. 1951. "Calculation of stresses in wire ropes," *Wire and Wire Products*, Vol. 26, pp. 766-767, 799-801.

Hruska, F. H. 1952. "Radial forces in wire ropes," *Wire and Wire Products*, vol. 27, No. 5, pp. 459-463.

Hruska, F. H. 1953. "Tangential forces in wire ropes," *Wire and Wire Products*, Vol. 28, No. 5, pp. 455-460.

Huang, X. and Vinogradov, O. 1992. "Interwire slip and its influence on the dynamic properties of tension cables," *Proceedings of the Second International Offshore and Polar Engineering Conference San Francisco, USA,* pp. 392-396.

Huang, X. and Vinogradov, O. 1994. "Analysis of dry friction hysteresis in a cable under uniform bending," *Structural Engineering and Mechanics,* Vol. 2, No. 1, pp. 63-80.

Huang, X. and Vinogradov, O. 1996. "Extension of a cable in the presence of dry friction," *Structural Engineering and Mechanics,* Vol. 4, No. 3, pp. 313-329.

Huang, X. and Vinogradov, O. 1996. "Dry friction losses in axially loaded cables," S*tructural Engineering and Mechanics,* Vol. 4, No. 3, pp. 330-344.

Knapp, R. H. 1979. "Derivation of a new stiffness matrix for helically armoured cables considering tension and torsion," *International Journal for Numerical Methods in Engineering,* Vol. 14, pp. 515-529.

Knapp, R. H. 1988. "Helical wire stresses in bent cables," *Journal of Offshore Mechanics and Arctic Engineering,* Vol. 110, No. 1, pp. 55-61.

Leissa, A. W. 1959. "Contact stresses in wire ropes," *Wire and Wire Products*, Vol. 34, No. 3, pp. 307-314, 372-373.

LeClaire, R. A. 1989. "Upper bound to mechanical power transmission losses in wire rope," *Journal of Engineering Mechanics-ASCE.* Vol. 115, No. 9, pp. 2011-2019.

LeClaire, R. A. 1991. "Axial response of multilayered strands with compliant layers," *Journal of Engineering Mechanics-ASCE.* Vol. 117, No. 12, pp. 2884-2903.

Love, A. E. H. 1944. "A treatise on the mathematical theory of elasticity," *Dover Publications Inc., New York.*

Machida, S. and Durelli. A. J. 1973. "Response of a strand to axial and torsional displacements," *Journal of Mechanical Engineering Science,* Vol. 15, pp. 241-251.

Miller, S. E., and Chynoweth, A. G. 1979. "Optical fiber telecommunications," *Academic Press Inc.*

Ogai, M., Hiramatsu, H., Oda, M., Kamata, Y., Miajima, Y., and Ieshigo, M. 1985. "Long-term reliability of optical fiber composite ground wire," *Proceedings of International Wire and Cable Symposium 34th.* Published by US Army, Fort Monmouth, NJ, USA. pp. 92-96.

Park, Y. B., Yoon, J. H., and Yang, D. Y. 1994. "Finite element analysis of steady-state three-dimensional helical extrusion of twisted sections using recurrent boundary conditions," *International Journal of Mechanical Science,* Vol. 36, No. 2, pp. 137-148.

Phillips, J. W. and Costello, G. A. 1973. "Contact stresses in twisted wire cables," *Journal of the Engineering Mechanics Division, Proceedings of the American Society of Civil Engineers.* Div. 99, pp. 331-341.

Ramsey, H. 1990. "Analysis of interwire friction in multilayered cables under uniform extension and twisting," *International Journal of Mechanical Science,* Vol. 32, No. 8, pp. 709-716.

Raoof, M. 1991. "Wire recovery length in a helical strand under axial-fatigue loading," *International Journal of Fatigue,* Vol. 13, No. 2, pp. 127-132.

Raoof, M. and Hobbes, R., E. 1988. "Analysis of Multilayered Structural Strands," *Journal of Engineering Mechanics,* Vol. 114, No. 7, pp. 1166-1182.

Raoof, M. and Huang, Y., P. 1992. "Wire stress calculations in helical strands undergoing

bending," *Journal of Offshore Mechanics and Arctic Engineering,* Vol. 114, No. 3, pp. 212-219.

Raoof, M. and Kraincanic, I. 1994. "Critical examination of various approaches used for analyzing helical cables," *Journal of Strain Analysis for Engineering Design,* Vol. 29, No. 1, pp. 43-55.

Raoof, M. and Kraincanic, I. 1995. "Simple derivation of the stiffness matrix for axial/torsional coupling of spiral strands," *Computers and Structures,* Vol. 55, No. 4, pp. 589-600.

Rabinowicz, E. 1995. "Friction and wear of materials," *John Wiley & Sons, Inc.*

Russ, C. R., Misono, N. Okazato, A. and Kobayashi, T. 1986. "Composite ground wire with optical fibers," *Proceedings of 35th International Wire and Cable Symposium,* Published by US Army Communications-Electronics Command, Fort Monmouth, NJ, USA. pp. 484-489.

Sathikh, S. 1989. "Effect of interwire friction on transverse vibration of helically stranded cable," *American Society of Mechanical Engineers, Design Engineering Division.* Published by ASME, New York, Vol. 18-4, pp. 147-153.

Savadjiev, K. and McComber, P. 1995. "Mechanical behavior of ice loaded optical ground wires," *Arctic/Polar Technology ASME.* Vol. IV, OMAE, pp. 107-113.

Schneider, H. W., Schobert, A., and Staudt A. 1987. "Influence of drawing conditions on the tensile strength of fluoride glass optical fibers," *Glastechnische Berichte,* Vol. 60, No. 6, pp. 205-210.

Singh, H. and Sirkis, J. S. 1993. "Strain analysis of thick and thin composites with embedded optical fibers under compression," *Experiments in Smart Materials and Structures, American Society of mechanical Engineers, Applied Mechanics division, AMD.* Published by ASME, New York, Vol. 181, pp. 39-46.

Suhir, E. 1993. "The effect of the nonlinear stress-strain relationship on the mechanical behavior of optical glass fibers," *International Journal of Solids and Structures.* Vol. 30, No. 7, pp. 947-961.

Suhir, E. 1995. "Fiber optics structural mechanics," *Proceedings of the Electronic Components and Technology Conference, IEEE, Piscataway, NJ, USA,* 95CH35820, pp. 937-948.

Szentesi, O. I. 1986. "Reliability of optical fibers, cables, and splices," *IEEE Journal on Selected Areas in Communications.* No. 9, pp. 1502-1508.

Velinsky, S. A., Anderson, G. L. and Costello, A. G. 1984. "Wire rope with complex cross-sections," *Journal of the Engineering Mechanics Division, Proceedings of the American Society of Civil Engineers.* Div. 110, pp. 380-391.

Uttings, W. S. and Jones, N. 1987. "The response of wire rope strands to axial tensile loads-Part I. Experimental results and theoretical predictions," *International Journal of Mechanical Science,* Vol. 29, No. 9, pp. 605-619.

Uttings, W. S. and Jones, N. 1987. "The response of wire rope strands to axial tensile loads-Part II. Comparison of experimental results and theoretical predictions," *International Journal of Mechanical Science,* Vol. 29, No. 9, pp. 621-636.

Ura, A., Nakashima, A., Yamamoto, Y., Kawazoe, T. 1991. "Friction properties of a wire rope for a cable puller," *International Conference on Wear of Materials,* Published by ASME, New York, NY, USA. Vol. 2, pp. 651-654.